A Description of the $\pi^-p \to NK\bar{K}$ Reaction in the Generalized Veneziano Model

YU. A. BUDAGOV, V. B. VINOGRADOV, L. L. ENKOVSKIĬ[1], S. V. KLIMENKO[2], V. V. KUKHTIN[1], N. K. KUTSIDI[3], G. MARTINSKA, AND V. V. TIMOKHIN[4]

Joint Institute for Nuclear Research

Submitted July 31, 1971

Zh. Eksp. Teor. Fiz. 62, 836-843 (March, 1972)

The $\pi^-p \to pK^-k^0$ and $\pi^-p \to \eta K^0\bar{K}^0$ reactions at 1.5–8 GeV/c are investigated within the framework of the generalized Veneziano model. The total and differential cross sections, effective mass distributions, and angular distributions of the secondary particles are calculated. The predictions are compared with the experimental data.

AT the present time, the most general dynamic model for inelastic processes of the type $1+2 \to 3+4+5$ is the generalized Veneziano model.[1] This is a dual model and combines the properties of the Regge amplitude at high energies and the amplitude with resonant poles at low energies. In this paper we use the generalized Veneziano model to analyze the process $\pi^-p \to NK\bar{K}$ (the reaction $\pi^-p \to pK^-K^0$ and $\pi^-p \to nK^0\bar{K}^0$) in the incident-pion energy range 1.5–8 GeV. Preliminary results of this investigation were reported at the 15th International Conference on High-Energy Physics (Kiev, 1970) and were published in the form of a preprint.[2]

1. THE MODEL

In the generalized Veneziano model, the amplitude of the process $1+2 \to 3+4+5$ is

$$A = \sum_{1}^{12} KB_5(x_{12}, x_{23}, x_{34}, x_{45}, x_{51}),$$

where B_5 is a five-point function[1] (the generalization of the Veneziano amplitude to five particles); $x_{ij} = J - \alpha_{ij}(s_{ij})$; α_{ij} is the linear Regge trajectory connected with the system of particles i and j; $s_{ij} = (p_i + p_j)^2$, and p_i and m_i are the four-momentum and mass of the i-th particle. The coefficient J is equal to the spin of the first particle on the trajectory at $s_{ij} > (m_i + m_j)^2$ and is equal to unity at $s_{ij} < (m_i + m_j)^2$. Such a choice of J in the resonance region ensures a correct connection between the masses and spins of the resonances, and corresponds in the scattering region to exchange of extra mesons and baryons in the ground P state. The kinematic factor K is chosen in the form

$$K = \varepsilon_{\alpha\beta\gamma\delta} P_1^{\alpha} P_2^{\beta} P_3^{\gamma} P_4^{\delta}.$$

The trajectories $\alpha(s)$ are specified in the form

$$\alpha(s) = \alpha_0 + \alpha' s + ia(s - s_0)^{\beta} \quad \text{for } s > s_0,$$
$$\alpha(t) = \alpha_0 + 0{,}9t \quad \text{for } s < s_0,$$

for $s > s_0$ and $\alpha(t) = \alpha_0 + 0.9t$ at $s < s_0$, where α_0, α', a, and s_0 are constants determined from the masses and widths of the resonances, and also from the results of experiments on hadron scattering.[3] The values of these constants for the employed trajectories are listed in the table. $\beta = \frac{1}{2}$ for the ρ-meson trajectory and $\beta = 1$ for the remainder.

a) The Reaction $\pi^-p \to pK^-K^0$

For the reaction

$$\pi^-p \to pK^-K^0, \tag{1}$$

eight out of the 12 diagrams contain channels with exotic quantum numbers and make no contribution to the amplitude.

The remaining four diagrams are shown in Fig. 1. The dominant trajectory is indicated in each two-particle channel. The choice of the K* trajectory in the $K\pi$ channel, the A_2 trajectory in the K^0K^- channel, or the Λ trajectory in the pK^- channel is governed by the quantum numbers of the systems and by the experimental information on the presence of the resonances K*, A_2, and $\Lambda(1520)$ in the corresponding effective-mass spectra.

The choice of the ω trajectory in the $\bar{p}p$ system is dictated by the behavior of the total and differential cross sections for the crossing process $K^+p \to K^0p\pi^+$.[4-6]

In the direct π^-p channel, alternative trajectories are N and Δ. Our choice of the N trajectory is arbitrary, but it does not affect the final result significantly. The reason is that the difference between the contributions of the N and Δ trajectories is small, owing to the large values of s_{ij} and the approximate equality of the slopes of these trajectories.[7]

Diagram d (Fig. 1) differs from diagram a or b in that only two external particles, connected with the K*–K** trajectory, are interchanged. The hypothesis of exchange degeneracy of K* and K** forbids simultaneous appearance of such diagrams in the amplitude, since the universality of the residues would lead to cancellation of every other pole on this trajectory. It is therefore necessary to choose between diagram d and the group of diagrams a and b. Since diagram d does not describe the production of the A_2 resonance in the K^0K^- system, we shall use diagrams a and b.

Taking into account the requirement of crossing symmetry of the amplitude and the absence of resonances N and Δ with negative signature, we should add diagrams a, b, and c with equal weights (diagram c, which is important for crossing reactions, differs from a and b in that only two particles connected with N and Δ trajec-

[1]Institute of Theoretical Physics, Ukrainian Academy of Sciences, Kiev.
[2]Institute of High Energy Physics, Serpukhov.
[3]Tbilisi State University.
[4]Kiev State University.

Parameters of trajectories

Trajectory	Below threshold	Above threshold	Trajectory	Below threshold	Above threshold
ρ	0.57+0.9t	—	N	—	−0.39+1.01s + + i·0.12(s − 1.14)
ω	0.40+0.9t	—			
A_2	—	0.45+0.89s + + i·0.10(s − 0.17)	Δ	0.12+0.9t	—
			Λ	—	−0.71+0.97s + + i·0.09(s − 1.77)
K*	0.34+0.9t	—			
			Y_1^*	−0.25+0.9t	—

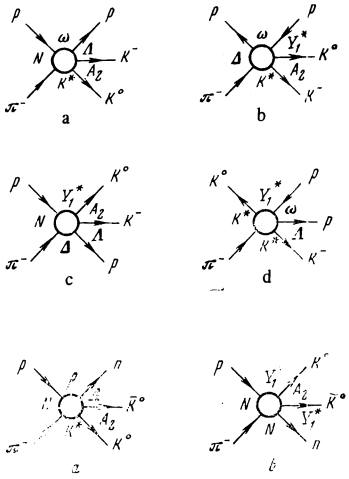

FIG. 1. Diagrams for the process $\pi^- p \to pK^- K^0$.

FIG. 2. Diagrams for the process $\pi^- p \to nK^0 \bar{K}^0$.

tories are interchanged). To simplify the calculations we have neglected diagram c, which contains only baryon exchange, and whose contribution is small compared with that of the meson exchange. The amplitude of the reaction (1) therefore takes the form

$$A = \gamma K\{(a) + (b)\},$$

where γ is a normalization parameter,

$$(a) = B_5[1/2 - \alpha_N(s_{12}),\ 1 - \alpha_\omega(t_{23}),\ 1/2 - \alpha_\Lambda(s_{34}),\ 1 - \alpha_{A_2}(s_{45}),\ 1 - \alpha_{K^*}(t_{51})],$$

$$(b) = B_5[1 - \alpha_\Delta(t_{12}),\ 1 - \alpha_\omega(t_{23}),\ 1 - \alpha_{Y_1^*}(t_{31}),\ 1 - \alpha_{A_2}(s_{45}),\ 1 - \alpha_{K^*}(t_{51})].$$

b) The Reaction $\pi^- p \to nK^0\bar{K}^0$

For the reaction

$$\pi^- p \to nK^0\bar{K}^0 \qquad (2)$$

there is no exchange of exotic trajectories only in two diagrams (Fig. 2). We neglect diagram 2b, which contains baryon exchange.

The amplitude of reaction (2) is thus

$$A_2 = \gamma K B_5[1/2 - \alpha_N(s_{12}),\ 1 - \alpha_\rho(t_{23}),\ 1/2 - \alpha_\Lambda(s_{34}),\ 1 - \alpha_{A_2}(s_{45}),\ 1 - \alpha_{K^*}(t_{51})].$$

2. COMPARISON OF THE PREDICTIONS OF THE MODEL WITH EXPERIMENT

To obtain the predictions, the amplitudes A_1 and E_2 were integrated over phase space by the Monte Carlo method with the aid of the FOWL program.[8] The functions B_5 were calculated in accordance with the Hopkinson program.[9] The errors of the calculations amounted to not less than 3% for the total cross sections and 8% for the differential cross sections. The results of the calculations are shown by the continuous curves in Figs. 3–8. The experimental data shown in these figures were taken from [10–15].

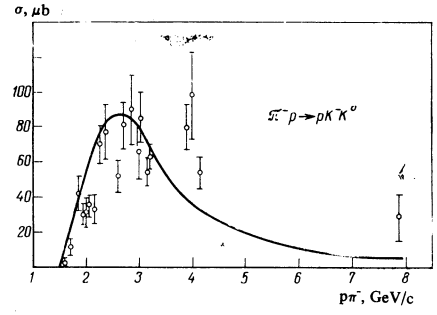

FIG. 3. Dependence of the cross section of the reaction $\pi^- p \to pK^- K^0$ on the momentum of the incident π^- meson.

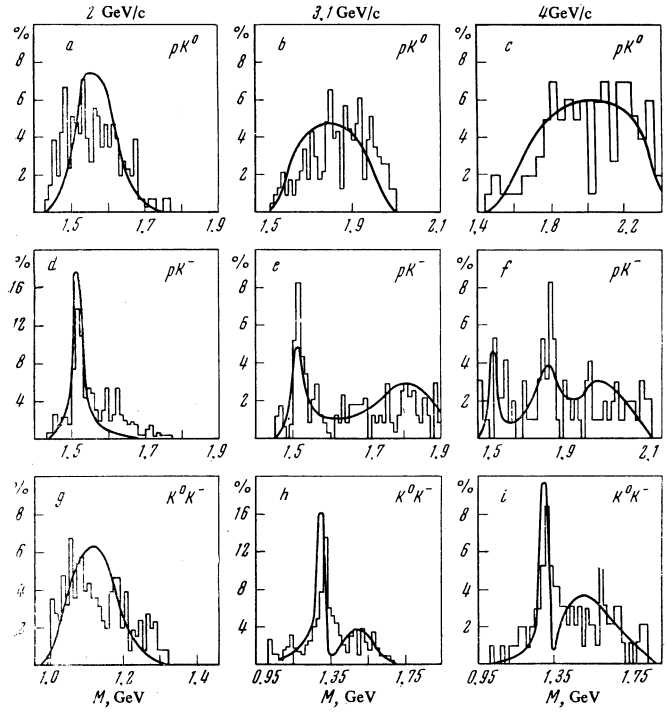

FIG. 4. Effective-mass distributions for the reaction $\pi^- p \to pK^- K^0$ at 2, 3.1, and 4 GeV/c.

a) The Reaction $\pi^- p \to pK^- K^0$

Figure 3 shows the predictions of the model for the dependence of the total cross section of the reaction (1) on the momentum of the incoming π^- meson. As seen from this figure, the model describes qualitatively correctly the behavior of the cross section with the change of energy.

Figure 4 shows the effective-mass distributions of the systems pK^0, pK^-, and K^0K^- for this reaction. The predictions of the model, namely the absence of resonances in the pK^0 system and the resonant structure in

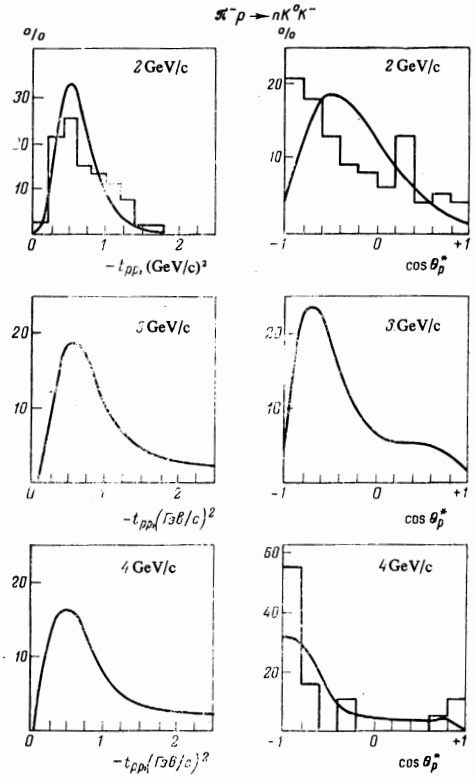

FIG. 5. Distributions with respect to the momentum transfer and the cosine of the proton emission angle in the c.m.s. for the reaction $\pi^- p \to pK^-K^0$.

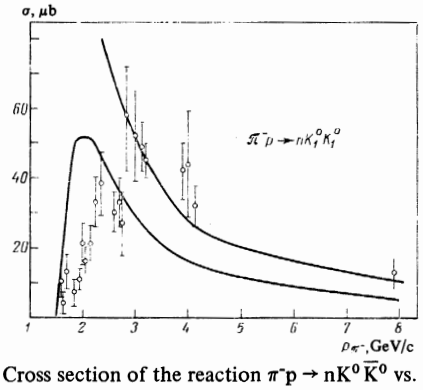

FIG. 6. Cross section of the reaction $\pi^- p \to nK^0\bar{K}^0$ vs. the momentum of the incident π^- meson.

the pK^- and K^0K^- systems agree satisfactorily, in the main, with experiment. The predicted probabilities of formation of the resonances $\Lambda(1520)$ and $A_2(1320)$ agree with the experimental ones within the limits of errors.

Figure 5 demonstrates the predictions of the model for the distributions with respect to the momentum transfer and the cosine of the proton emission in the c.m.s. of the primary interaction. The model predicts a peripheral interaction and an increase of the anisotropy of the proton emission with increasing incident-pion energy.

Thus, the model describes satisfactorily, in the main, the basic characteristics of the reaction $\pi^- p \to pK^-K^0$ at incident pion energies 1.5–8 GeV.

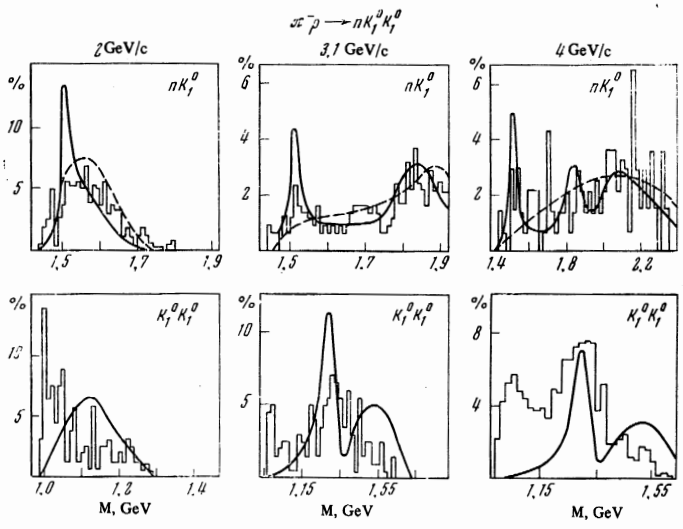

FIG. 7. Effective-mass distributions of the systems nK_1^0 and $K_1^0K_1^0$ for the reaction $\pi^- p \to nK^0\bar{K}^0$.

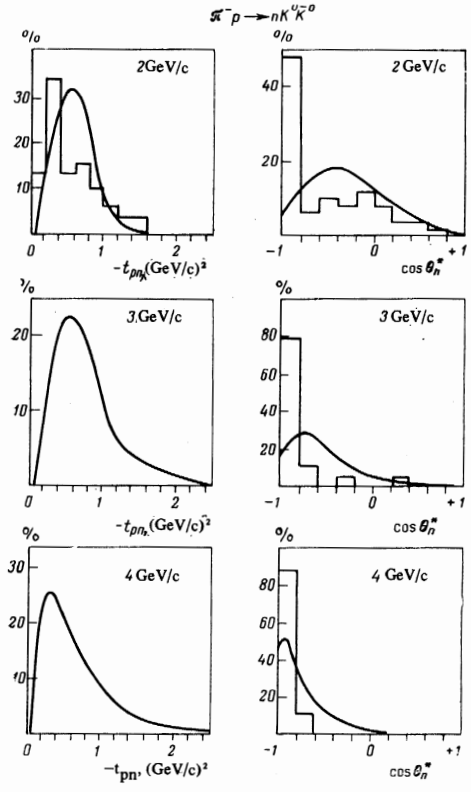

FIG. 8. Distributions with respect to the momentum transfer and the cosine of the neutron emission angle in the c.m.s. for the reaction $\pi^- p \to nK^0\bar{K}^0$.

b) The Reaction $\pi^- p \to nK^0K^0$

Figure 6 shows the dependence of the cross section of the reaction (2) on the momentum of the incident π^- mesons. The curves on this figure correspond to two different values of the normalization parameter γ. As seen from the figure, the predictions agree with experiment, starting only with an energy ~3 GeV.

Figure 7 shows the distributions with respect to the effective masses of the system nK_1^0 and $K_1^0K_1^0$. Since the calculations were performed for the final state $nK^0\bar{K}^0$, the histograms of nK^0 and $n\bar{K}^0$ were added to obtain the nK_1^0 distribution. These histograms are shown by the continuous line. The dashed curve shows the distribution with respect to the effective mass of the system nK^0, in which no resonances are produced. The dashed curve describes the general behavior of this distribution but does not predict formation of resonances. On the other hand, the summary distribution (continuous line) predicts the formation of resonances. However, the predictions do not agree quantitatively with experiment. As to the $K_1^0K_1^0$ spectrum, its complicated resonant structure (threshold anomaly at $M \sim 1000$ MeV and interference of f and A_2 mesons) cannot be described within the framework of the present model (Fig. 7).

Figure 8 shows, for the reaction (2), the distributions with respect to the momentum transfer and the cosine of the neutron emission angle in the c.m.s. of the primary interaction at different incident-pion energies. As seen from this figure, the model predicts the peripheral character of the interactions, but the predictions are in poor quantitative agreement with experiment.

It is thus impossible to describe correctly the characteristic features of the reaction $\pi^-p \to nK^0\bar{K}^0$ within the framework of the employed model.

In conclusion we note that Chan et al.[6] described the reaction (1) simultaneously with the two crossing-symmetry reactions $K^+p \to K^0\pi^+$ and $K^-p \to \bar{K}^0\pi^-p$ with the aid of a single amplitude. Following the publication of our preliminary results,[2] Collins et al.[7] and Hoyer et al.[16] reported investigations of the reaction (2). This reaction was analyzed in [7] at $p = 12$ GeV/c in the double Regge region ($s_{ij} > 3.5$ GeV^2); Hoyer[16] considered the effective masses in the A_2–f resonance region. The conclusions of these investigations do not contradict our results.

We are grateful to V. P. Dzhelepov and V. P. Shelest for constant interest and help with the work, and to V. B. Flyagin, A. G. Volod'ko, V. I. Zhuravlev, and B. V. Struminskiĭ for useful discussions.

[1]K. Bardakci and H. Ruegg, Phys. Lett. B **28,** 342 (1968); M. Virasoro, Phys. Rev. Lett. **22,** 37 (1969).
[2]L. L. Jenkovsky, V. V. Kukhtin, and V. V. Timokhin, Preprint ITP 70–77, Kiev, 1970.
[3]D. V. Shirkov, JINR Preprint R2-4726, Dubna, 1969.
[4]D. R. Morrison, Phys. Lett. **22,** 528 (1966).
[5]G. Bellettini, Rapporteur's talk, XIV ICHEP, Vienna, 1968.
[6]Chan Hong-Mo, R. O. Raito, G. H. Thomas, and N. A. Tornqvist, Nucl. Phys. B **19,** 173 (1970).
[7]P. A. Collins, B. J. Hartley, R. W. Moore, and K. J. M. Moriarty, Nucl. Phys. B **22,** 150 (1970).
[8]F. James, FOWL, CERN Program Library, W505, 1965.
[9]J. F. Hopkinson, Preprint DNPL/p21, Daresbury, 1969.
[10]O. I. Dahl, L. M. Hardy, R. I. Hess, J. Kirz, and D. H. Miller, Phys. Rev. **163,** 1377 (1967).
[11]R. Ehrlich, W. Selove, and H. Yuta, Phys. Rev. **152,** 1194 (1966).
[12]G. Alexander, O. I. Dahl, L. Jacobs, G. R. Kalbfleisch, D. H. Miller, A. Rittenberg, J. Schwartz, and G. A. Smith, Phys. Rev. Lett. **9,** 460 (1962).
[13]J. Bartsch, L. Bondar, R. Speth, G. Hotop, G. Knies, R. Storim, J. M. Brownlee, N. N. Biswas, D. Lüers, N. Schmitz, R. Seeliger, and G. P. Wolf, Nuovo Cimento A **43,** 1010 (1966).
[14]T. F. Hoang, D. P. Eartly, J. J. Phelan, A. Roberts, C. L. Sandler, S. Bernstein, S. Margulies, D. W. McLeod, T. H. Groves, N. N. Biswas et al, Phys. Rev. **184,** 1363 (1969).
[15]T. P. Wangler, A. R. Erwin, and W. D. Walker, Phys. Rev. **137,** 414 (1965).
[16]P. Hoyer, B. Petersson, A. T. Lea, J. E. Paton, and G. H. Thomas, Preprint CERN, TH-1262, Geneva, 1970.
[17]B. Petersson and N. A. Tornqvist, Nucl. Phys. B **13,** 629 (1969).

Translated by J. G. Adashko
100